Optimization of GND Contact Placements for Cavity Resonance Suppression

Jan Krummenauer[#1], Yuming Du[#2], Nesrine Kammoun[#3], Jürgen Götze [*#4]
[#]Cross-Domain Computing Solutions, Robert Bosch GmbH, Germany
[*]Information Processing Lab, TU Dortmund, Germany
{[1]Jan.Krummenauer, [2]Yuming.Du,[3]Nesrine.Kammoun}@de.bosch.com, [4]Jürgen.Götze@tu-dortmund.de

***Abstract*— Noise currents coupling into the housing of automotive ECUs can stimulate cavity resonances, leading to increased levels of crosstalk or increased electromagnetic radiation in critical frequency ranges. A cost effective countermeasure to reduce such unwanted resonances is the placement of spring contacts, which provide additional GND connections inside the housing. However, an ideal placement of these contacts is difficult to find, as evaluating the exact effects of contact placements requires a costly 3D FEM simulation. In this paper we present a computationally efficient method to find optimized placement positions of spring contacts for resonance suppression. By generating a grid of ports in a 3D simulation setup and by improving the post-processing of the resulting S-Parameter matrix, we significantly reduce the required computation effort for evaluating different spring placements. This enables the application of optimization algorithms and a fast visualization of the cavity resonant modes. Using measurements, we validate our simulation results and observe a damping effectiveness for the resonance peaks of up to 18 dB.**

***Keywords*— cavity resonances, resonance suppression, housing resonance, genetic algorithm, spring contacts, absorber sheets**

I. Introduction

Automotive ECUs are typically housed in aluminum enclosures, which have a high electrical and thermal conductivity, providing effective heat transfer and electromagnetic shielding. However, noise currents coupling into the conductive housing can stimulate cavity resonances, which can result in unwanted electromagnetic interference (EMI) in critical frequency ranges, e.g. near GLONASS and GPS bands at around 1.6GHz [1]. The noise current typically couples capacitively into the housing, for example originating from large integrated circuits (IC) that are placed under heat sink sections of the housing (see Figure 1). If noise frequencies match with cavity resonance frequencies, resonant modes amplify the noise signals. This leads to higher levels of crosstalk within the ECU and to increased electromagnetic emissions, which can, for example, radiate via slots at the clamping edges of the housing caused by mechanical tensions.

The resonant frequencies are determined by the dimensions of the housing and can be approximated using the formula below which is valid for rectangular cavities [2]:

$$f_{mnl} = \frac{c}{2\sqrt{\mu_r \epsilon_r}} \sqrt{\left(\frac{m}{a}\right)^2 + \left(\frac{n}{b}\right)^2 + \left(\frac{l}{d}\right)^2} \qquad (1)$$

where a, b, d are the dimensions of the rectangular cavity and m, n, l are the mode numbers (e.g. 1,1,0 for TE_{110} mode). A precise estimation of these resonant frequencies, however, requires runtime intensive 3D FEM simulations.

A typical EMC countermeasure for damping unwanted resonant modes in cavities are absorber sheets [3], [4]. Yet, the use of such sheets is often limited by the need for thermal connections from the PCB to the enclosure for cooling purposes. Other proposed countermeasures involve changing the shape of the housing, e.g. by placing pins in the housing [5] or placing a grounded bar in the middle of the housing [6]. Rather than directly suppressing the resonant modes, other proposed countermeasures are to prevent known noise sources from stimulating the resonant modes, e.g. by placing grounded cages around critical ICs, as suggested by [7]. However, all of the above mentioned countermeasures involve high costs, or must be implemented in an early stage of the design process.

A more cost effective and easier to implement solution is the placement of contact springs (e.g. [8]), which are commonly used for GND connections in between PCB's or for EMC shielding in the region of housing openings. The placement of these spring contacts as ground (GND) connection or in combination with series resistors has a direct impact on the housing resonance behavior.

In this paper we propose a method to efficiently optimize placement configurations for the spring contacts and to visualize their impact on the different resonant modes. Instead of running multiple costly 3D FEM simulations with different port positions for multiple placement configurations, we propose to define a grid of ports and run only a single 3D simulation. This allows the evaluation of different spring placements using post-processing only. Further, we accelerate post-processing by a factor of 500 using a Z-parameter conversion. This improved post-processing enables us to apply optimization algorithms, such as a Genetic Algorithm (GA) to

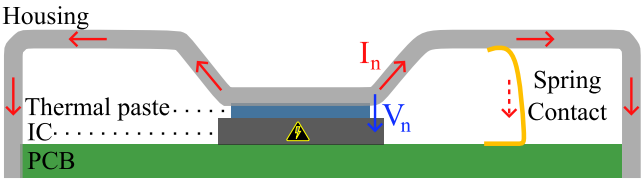

Fig. 1. The capacitive coupling of noise current into the housing stimulating cavity resonances. Spring contacts can suppress these resonances for certain frequencies.

the problem and to efficiently visualize the effects of the spring contacts on the resonant modes.

Section II introduces the simulation steps necessary to evaluate the housing resonances and the effects of different spring placements. Next, the optimization setup and optimization results are presented in section III. Subsequently, section IV provides measurement results, which validate our simulation based optimization outcome, showing a resonance peak suppression of up to 18dB.

II. Efficient evaluation of spring contact impact on housing resonances

Considering an ECU housing as shown in Figure 2.a), our goal is to evaluate the cavity resonances in between the PCB, which is in the simulation modeled as a filled GND-plane, and the top-side of the housing. A typical approach would be to define a 3D simulation setup with the shown configuration, and a small number of ports for noise stimulation, resonance measurements, e.g. by using antennas, and possible spring contact positions. Such a 3D simulation has a runtime T_{3D} in the range of hours (e.g. $T_{3D} = 1h41m$ in our example). When analyzing multiple spring contact configurations this simulation is often repeated with different port positions, resulting in an inefficient evaluation process with a total runtime of $T_R = m \cdot T_{3D}$ for a number of m evaluations.

To more efficiently estimate the impact of different GND contact configurations for resonance suppression, we propose to place a *grid of ports* in the simulation setup. We automated the grid placement in CST Studio using the python API. All ports are placed vertically and are connected to the bottom GND-plane and the top of the housing. The 3D simulation with a port grid has a comparable runtime to a simulation with only a small number of ports ($T_{3D-grid} = 3h04m$).

After simulation, we obtain an n-port touchstone file. In this paper we consider a port grid with the size of 5x15, resulting in a 75-port touchstone file. For larger ECU dimensions or multilayer PCBs, the number of ports may further increase, resulting in a quadratically increasing size of the S-parameter matrix.

In a next step, spring contacts and resistors can be cascaded to the n-port using post-processing. When using CSTs standard post-processing, the resonance evaluation has a significant runtime of $T_{PP} = 60s$ for the 75-port S-parameter matrix. When using a denser port grid with 150 ports, this runtime rises significantly to $T_{PP} = 10m$. The reason for this large runtime is that the post-processing is computed on the S-parameter matrix, where open-connections must be cascaded to all unused ports of the grid.

	Standard Simulation	**Port Grid + standard post-processing**	**Port Grid + Z-parameter post-processing**
Cumulative runtime T_R	$m \cdot T_{3D}$	$1 \cdot T_{3D-grid}$ $+m \cdot T_{PP}$	$1 \cdot T_{3D-grid}$ $+m \cdot T_{PP-Z}$
Runtime measurements	$m \cdot 1h41m$	$1 \cdot 3h04m$ $+m \cdot 60s$	$1 \cdot 3h04m$ $+m \cdot 0.12s$

Table 1. Comparison of cumulative runtime for m evaluations of the proposed method using Z-parameter post-processing and a 5x15 port-grid to the standard simulation approach and standard post-processing

As a large number of ports remain unused and open in this experiment, we propose a customized post-processing by converting the S-parameters to Z-parameters. Figure 2.b) shows the equivalent circuit for the n-port described by Z-parameters, which are defined as:

$$Z_{ab} = \left.\frac{V_a}{I_b}\right|_{I_k=0 \text{ for } k \neq b} \tag{2}$$

One advantage is that the Z-parameters can be used to directly observe the housing resonances. E.g., considering a noise source stimulating the housing at P_1 and all other ports remain open (no spring contact is placed), the housing resonances can be evaluated by observing Z_{11}, which describes the voltage on the housing at P_1 stimulated by the noise current coupling into P_1. The resulting noise voltage at other port locations P_k can also be evaluated by observing Z_{k1}, for resonances stimulated by I_1.

Additionally, the Z-parameter representation allows to easily simplify the n-port. When unused ports remain open their corresponding input current remains zero. Thereby, the Z-matrix can be reduced simply by removing the rows and columns of unused ports:

$$\begin{pmatrix} V_1 \\ \cancel{V_2} \\ \vdots \\ V_n \end{pmatrix} = \begin{pmatrix} Z_{11} & \cancel{Z_{12}} & \cdots & Z_{1n} \\ \cancel{Z_{21}} & \cancel{Z_{22}} & \cdots & \cancel{Z_{2n}} \\ \vdots & \vdots & \ddots & \vdots \\ Z_{n1} & \cancel{Z_{n2}} & \cdots & Z_{nn} \end{pmatrix} \begin{pmatrix} I_1 \\ \cancel{V_2} \\ \vdots \\ I_n \end{pmatrix} \tag{3}$$

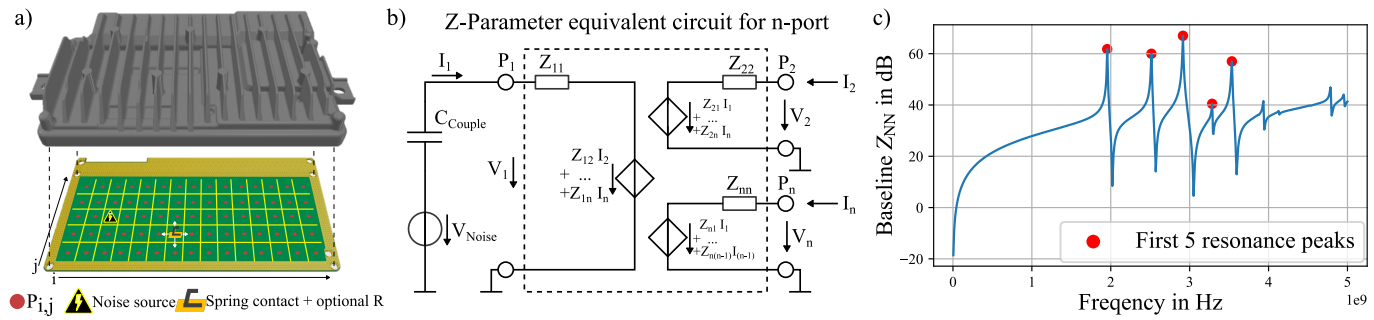

Fig. 2. a) Overview of Experiment Setup. b) Equivalent circuit of an n-port represented by its Z-parameters. A noise source is considered to capacitively couple into P_1. c) Baseline housing resonances. The plot shows Z_{NN}, which represents the voltage on the housing at P_N stimulated by the noise current.

Cascading the spring contacts and resistors to the reduced n-port matrix significantly accelerates the evaluation and reduces the runtime to $T_{\mathrm{PP-Z}} = 0.12s$. Table 1 summarizes the runtime of the different approaches, comparing the total runtime for a number of m evaluations.

III. Spring Placement Optimization

In the experiment below, we consider a single noise source in the housing at $P_{2,2} = P_{\mathrm{N}}$ (see Figure 2.a), which is the location of a large IC in the ECU. By evaluating the baseline housing resonances stimulated by a noise current at this port, we observe the resonance behaviour Z_{NN} as shown in Figure 2.c).

A. Optimization setup

Considering an allowed placement of two spring contacts with corresponding series resistors on the port grid, the input vector $\mathbf{x}$ consists of four input variables for optimization:

$$\mathbf{x} = \{P_{\mathrm{S0}}, P_{\mathrm{S1}}, R_{\mathrm{S0}}, R_{\mathrm{S1}}\} \tag{4}$$

where $P_{\mathrm{S0}}, P_{\mathrm{S1}}$ are the port positions for the spring contacts and $R_{\mathrm{S0}}, R_{\mathrm{S1}}$ correspond to the size of connected serial resistors.

The optimization objective is defined in such a way that the first 5 resonance peaks are suppressed as much as possible:

$$\min : O(\mathbf{x}) = \max(\mathbf{Z_{5P-B}}) - \max(\mathbf{Z_{5P}}(\mathbf{x})) \tag{5}$$

with $\mathbf{Z_{5P-B}}$ corresponding to the first 5 resonance peaks of the baseline spectrum and $\mathbf{Z_{5P}}(\mathbf{x})$ corresponding to the first 5 resonance peaks of an evaluation with inputs $\mathbf{x}$. The peaks with their amplitude in dB are found using scipy [9].

For the optimization, we use a Genetic Algorithm (GA), which is a standard black-box optimization method provided by pymoo [10]. We define a population size of 30 and a maximum number of experiment evaluations of 20,000. Further, we perform 10 optimization trials with different random seeds to compensate the statistical behavior of the optimization method.

While we consider a single noise source and the application of two spring contacts with serial resistors as countermeasure in the introduced experiment, the proposed post-processing method also provides a basis for other optimization setups. Such setups could for example consider multiple noise sources, leave-out-areas where spring placements are forbidden, varying numbers of springs, and other optimization objectives, e.g., by focusing on specific peaks or frequency regions.

B. Optimization results

Figure 3.a) shows the optimization convergence of the 10 optimization trials. The best value was found in 4 out of 10 trials:

$$O_{\min}(P_{(7,1)}, P_{(13,3)}, 30\Omega, 100\Omega) = -29.17 \text{ dB} \tag{6}$$

All trials show a convergence after multiple thousand runs, emphasizing the importance of the accelerated post-processing.

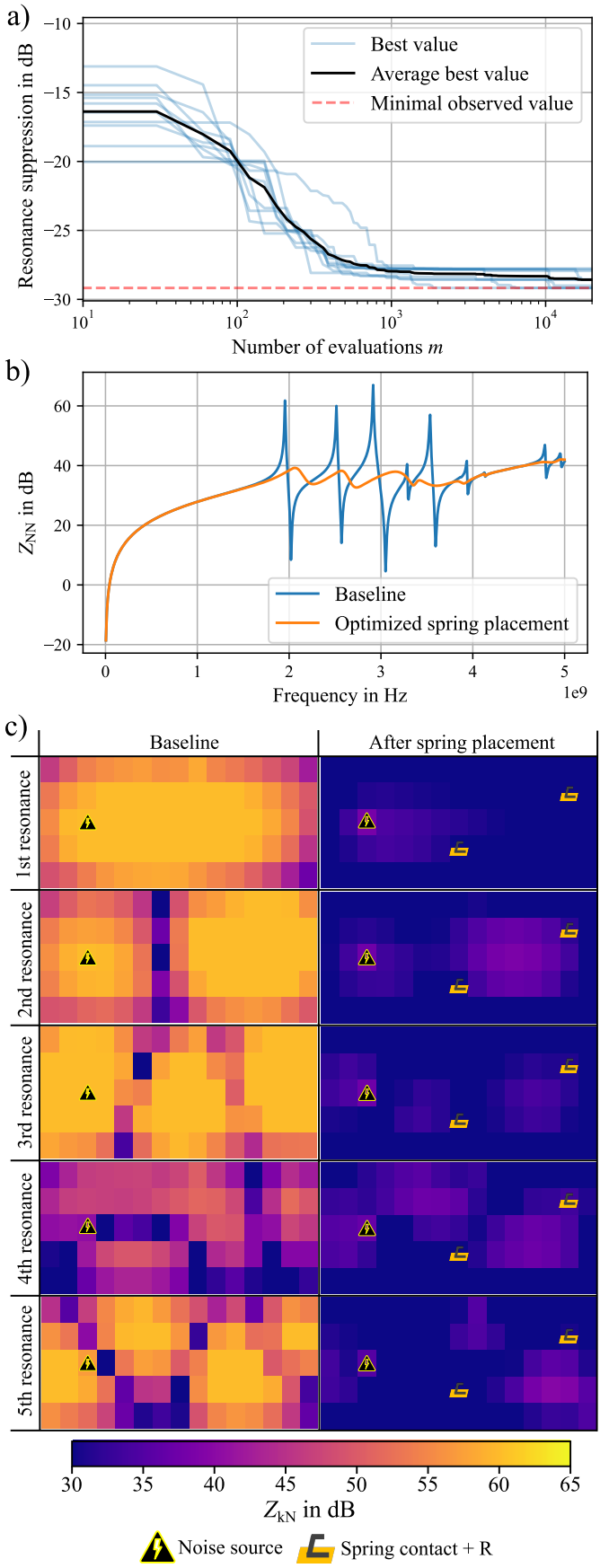

Fig. 3. a) shows the optimization convergence of the optimization trials. b) shows the comparison of the baseline cavity resonances to the resonance spectrum after placing the spring contacts in the optimized configuration. c) depicts the resonant modes inside the housing by showing Z_{kN} in a heatmap. This corresponds to the resulting voltage on each port on the grid stimulated by the noise current at P_{N}.

Figure 3.b) shows the comparison of the baseline resonance spectrum to the spectrum with applied springs as countermeasure. The plot shows a significant suppression of the resonant modes of up to 29 dB. Figure 3.c) provides deeper insights on the impact of spring contacts on the resonant modes, showing heatmaps of Z_{kN} at resonance peak frequencies. Z_{kN} represents the resulting noise voltage on all ports P_{k} on the grid, stimulated by the noise current at P_{N}. The different resonant modes in the baseline show similarities to modes encountered in perfect rectangular cavity resonators, however at higher frequencies the complexity of the field modes increases. The impact of the spring placement is shown on the right side, visually demonstrating the efficient suppression of the resonant modes.

IV. Measurements

We conducted measurements to validate our simulation results. Figure 4.a) shows the measurement setup. We connected the housing, closed by a PCB consisting mainly of a GND-Plane, via SMA-connectors to a Keysight E5071C Vector Network Analyzer (VNA), measuring S_{11}. We conducted a short-open-load (SOL) de-embeddeding, to eliminate the influence of the test-setup. Figure 4.b) shows the measured cavity resonances in comparison to simulation. The measurements match with the simulation results up to 3.5GHz. Small deviations of the resonance frequencies are caused by the measurement setup and by unavoidable inaccuracies when carrying out the de-embedding method. Using the spring contacts in the optimized configuration shows a suppression of the resonance peaks of up to 18 dB.

V. Conclusion

In this paper we propose a method to efficiently optimize the placement of spring contacts for the suppression of cavity resonances in ECU housings. By defining a grid of ports in a 3D simulation setup and by significantly improving post-processing steps using a Z-parameter conversion, we enable the application of optimization methods to the problem. The optimized spring contact configuration showed a damping effectiveness up to 18 dB in measurements, confirming the simulation results and the proposed approach for solving EMC issues. In addition to the results shown, this contribution provides a basis for further experiments, e.g. with different optimization setups, different optimization methods, or for the application of explainable AI methods to the problem.

Acknowledgment

This work is partly funded by the Bundesministerium für Wirtschaft und Klimaschutz (BMWK) of the Federal Republic of Germany as part of the research project progressivKI (https://www.edacentrum.de/projekte/progressivKI) in the funding programme NFST (Grant number 19A21006O). The responsibility for this publication is held by the authors only.

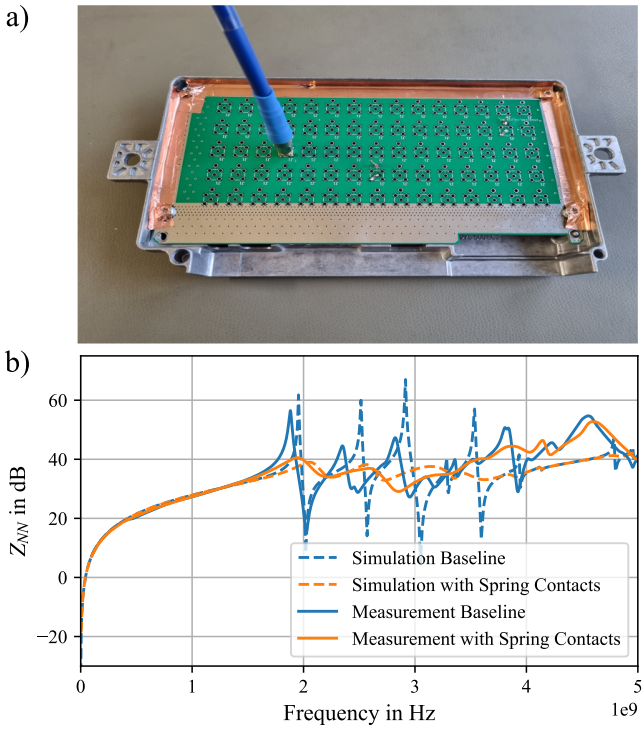

Fig. 4. a) shows the measurement setup of the housing connected to the VNA via SMA connectors. b) shows the measured Z-parameters in comparison to the simulation results.

References

[1] G. M. Corporation, "General specification for electrical/electronic components and subsys-tems, electromagnetic compatibility, gmw3097," Dec. 2022. [Online]. Available: https://standards.globalspec.com/std/13263607/gmw3097

[2] S. Ramo, J. Whinnery, and T. Van Duzer, *Fields and Waves in Communication Electronics*. Wiley, 1994.

[3] P. Dixon, "Cavity-resonance dampening," *IEEE Microwave magazine*, vol. 6, pp. 74–84, 2005.

[4] P. Deroy, M. Koledintseva, C. Rostamzadeh, M. Worden, T. Monti, W. Schulz, and A. Ramanujan, "Effectiveness of noise suppressing sheet material for mitigation of automotive radiated emissions," *IEEE Transactions on Electromagnetic Compatibility*, vol. 63, no. 2, pp. 398–409, 2021.

[5] M. Nisanci, F. Hilmi, and P. De, "Efficient analytical prediction of the cavity resonant behavior of pec-pmc metallic enclosures and packages," *IEEE Transactions on Electromagnetic Compatibility*, vol. 63, pp. 93–102, 2020.

[6] S. Theepak, V. Namburi, B. Devadas, and R. Selvapriya, "Mitigation of resonance in rf high power amplifier enclosure," in *IEEE Topical Conference on RF/Microwave Power Amplifiers for Radio and Wireless Applications (PAWR)*. IEEE, 2017.

[7] C. Tong, *EMI Shielding Materials and Absorbers for 5G Communications*. Cham: Springer Nature Switzerland, 2022, pp. 143–172.

[8] M. M. T. C. GmbH, "Smd contact springs," Mar. 2024. [Online]. Available: https://www.mtc.de/en/emc-metal-parts/smd-contact-springs

[9] P. e. a. Virtanen, "Scipy 1.0: fundamental algorithms for scientific computing in python," *Nature Methods*, vol. 17, no. 3, pp. 261–272, Feb. 2020.

[10] J. Blank and K. Deb, "Pymoo: Multi-objective optimization in python," *IEEE Access*, vol. 8, pp. 89 497–89 509, 2020.